Supplementary Materials for

Research on NiMoTi Alloy Thin Film Hydrogen Evolution Catalysts via High-Throughput Screening Using Total Internal Reflection Imaging

Zi-Xin Wu,[a†] Xuan Xiao, [b†] Huang Chen,[a†] Zeng-Xian Fang,[a] Man-Zhen Lin,[b] Hao Lin,[a,c] Lian-Yu Li,[a] Huai-Yi Xu,[a] Jing-Yu Xi,[a] Dong-Zhi Li,[*d] Wei-Bing Liao*[b] and Le Liu*[a]

[a.]Shenzhen Key Laboratory of Advanced Layered Materials for Value-added Applications, Institute of Materials Research, Tsinghua Shenzhen International Graduate School, Tsinghua University, Shenzhen 518055, P. R. China.
[b.]Shenzhen Key Laboratory of Nuclear and Radiation Safety, College of Physics and Optoelectronic Engineering, Shenzhen University, Shenzhen 518060, China
[c.]Shenzhen Engineering Research Laboratory for Sludge and Food Waste Treatment and Resource Recovery, Tsinghua Shenzhen International Graduate School, Tsinghua University, Shenzhen 518055, P. R. China..
[d.]School of Advanced Manufacturing, Guangdong University of Technology, Jieyang 515200, P. R. China..
Co-first authors
† Zixin Wu, Xuan Xiao and Huang Chen contributed equally to this work and should be considered as co-first authors.

This PDF file includes:

Figs. S1 to S6
Tables S1 to S2

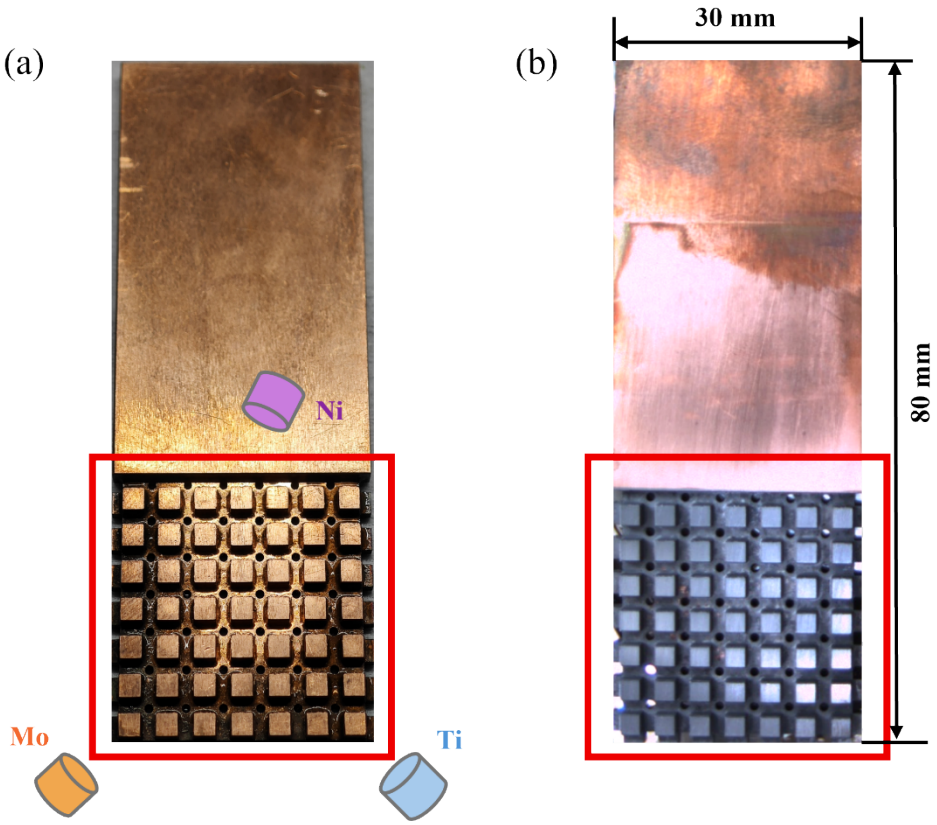

Fig. S1.
Copper electrodes (a) pre-deposition and (b) post-deposition of NiMoTi alloy films.

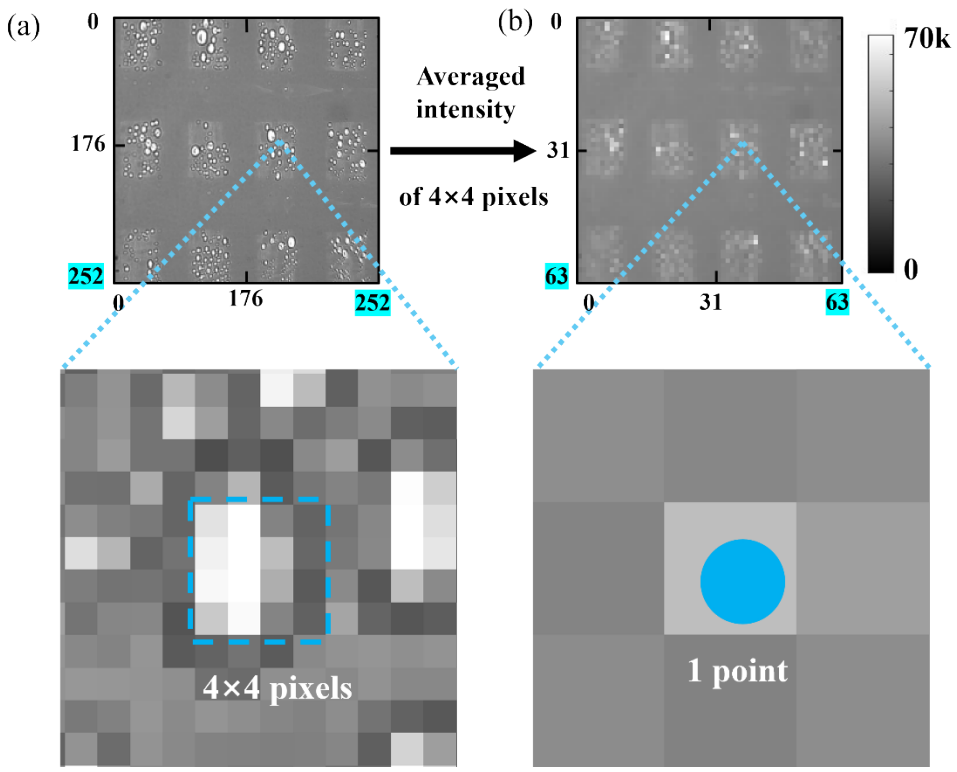

Fig. S2.

Electrode surface images captured by the camera system. (a) Image size: 252×252 pixels. (b) Image size: 63×63 points. To reduce optical intensity noise, the intensities of each 4×4 pixels were averaged into the intensity of 1 point, resulting in the 63×63-point image shown in fig. S2(b).

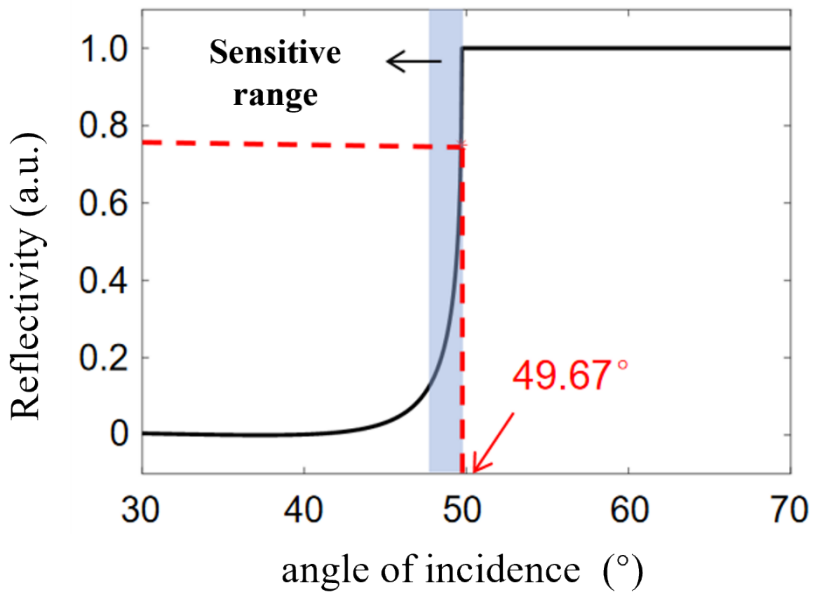

Fig. S3.
The relationship between reflectivity and the angle of incidence.

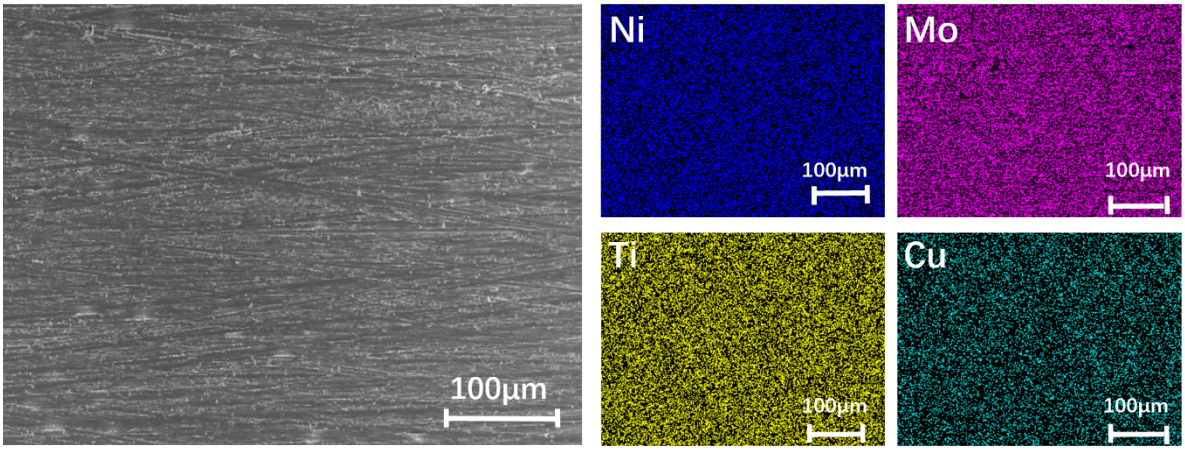

Fig. S4.

SEM image and elemental distribution maps of Ni, Mo, Ti, and Cu for the NiMoTi thin film.

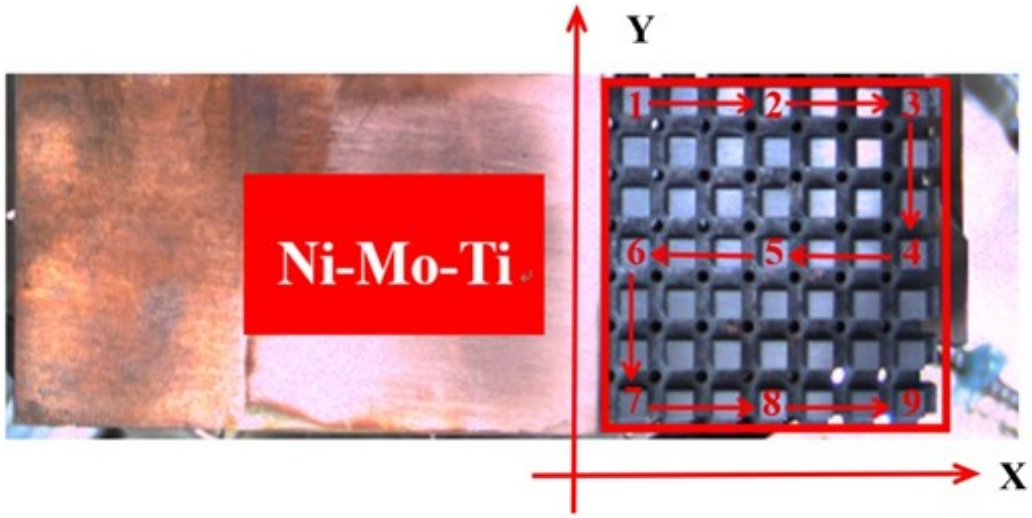

Fig. S5.

EDS scan path of NiMoTi thin films..

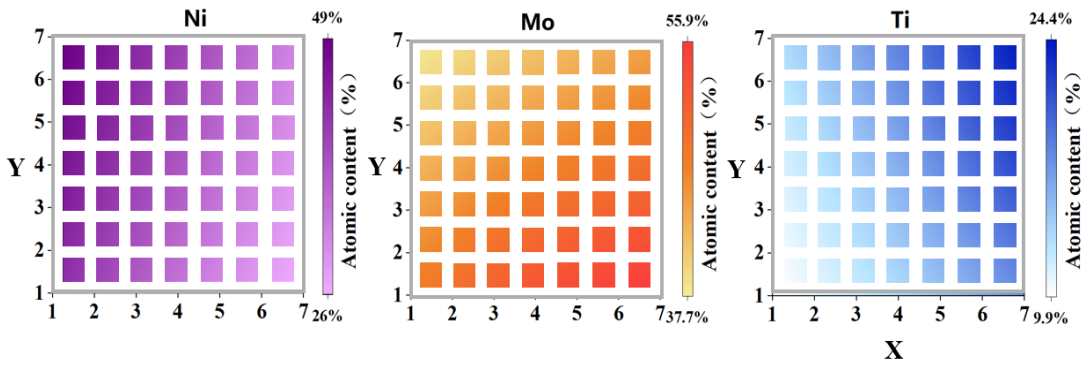

Figure S6.

Variations in Elemental Composition Across Different Regions of NiMoTi Thin Film Electrodes.

Table S1.

Compositional distribution of Ni, Mo, and Ti elements across different regions.

X	Y	Ni (at%)	Mo (at%)	Ti (at%)	X	Y	Ni (at%)	Mo (at%)	Ti (at%)
1	1	42.6	47.5	9.7	4	5	38.3	44.6	16.9
1	2	43.8	45.7	10.4	4	6	39.2	43.0	17.7
1	3	45.0	43.9	11.0	4	7	40.0	41.4	18.4
1	4	46.2	42.0	11.6	5	1	31.3	53.7	14.8
1	5	47.3	40.4	12.1	5	2	32.4	51.6	15.8
1	6	48.3	38.9	12.6	5	3	33.5	49.6	16.7
1	7	49.2	37.5	13.1	5	4	34.6	47.5	17.8
2	1	39.8	49.2	10.8	5	5	35.5	45.7	18.7
2	2	41.0	47.3	11.5	5	6	36.4	44.0	19.5
2	3	42.2	45.5	12.2	5	7	37.2	42.4	20.3
2	4	43.4	43.5	12.9	6	1	28.7	54.9	16.3
2	5	44.4	41.9	13.6	6	2	29.7	52.7	17.4
2	6	45.4	40.4	14.1	6	3	30.8	50.7	18.4
2	7	46.2	38.9	14.7	6	4	31.8	48.5	19.5
3	1	37.0	50.8	12.0	6	5	32.7	46.6	20.5
3	2	38.2	48.8	12.8	6	6	33.6	44.9	21.4
3	3	39.3	46.9	13.6	6	7	34.3	43.2	22.3
3	4	40.5	44.9	14.4	7	1	26.0	55.9	17.9
3	5	41.5	43.2	15.1	7	2	27.1	53.7	19.0
3	6	42.4	41.7	15.8	7	3	28.1	51.6	20.2
3	7	43.3	40.2	16.4	7	4	29.1	49.4	21.4
4	1	34.0	52.4	13.4	7	5	30.0	47.5	22.4
4	2	35.1	50.4	14.3	7	6	30.8	45.6	23.4
4	3	36.2	48.4	15.2	7	7	31.5	43.9	24.4
4	4	37.4	46.4	15.9					

Table S2.

Regional average onset potential distribution.

X	Y	Potential (V) vs. RHE	X	Y	Potential (V) vs. RHE
1	1	-0.23473	4	5	-0.22275
1	2	-0.22602	4	6	-0.22921
1	3	-0.22939	4	7	-0.23308
1	4	-0.21729	5	1	-0.22446
1	5	-0.22836	5	2	-0.21664
1	6	-0.22218	5	3	-0.22858
1	7	-0.23221	5	4	-0.22294
2	1	-0.22416	5	5	-0.21921
2	2	-0.21763	5	6	-0.22609
2	3	-0.21534	5	7	-0.23443
2	4	-0.21993	6	1	-0.22339
2	5	-0.22419	6	2	-0.22921
2	6	-0.22131	6	3	-0.23213
2	7	-0.23419	6	4	-0.22916
3	1	-0.21465	6	5	-0.23361
3	2	-0.2147	6	6	-0.23157
3	3	-0.21611	6	7	-0.23261
3	4	-0.20987	7	1	-0.24883
3	5	-0.22314	7	2	-0.23195
3	6	-0.22124	7	3	-0.23398
3	7	-0.22511	7	4	-0.21981
4	1	-0.2239	7	5	-0.23052
4	2	-0.21484	7	6	-0.23292
4	3	-0.21832	7	7	-0.23337
4	4	-0.22354			